Low pressure solubilities of CO_2 in guanidinium trifluoromethanesulfonate–MDEA systems

Nor Asrina Sairi [a,*], Noraini Abd Ghani [a], Mohamed Kheireddine Aroua [b], Rozita Yusoff [b], Yatimah Alias [a]

[a] Chemistry Department, Faculty of Science, University of Malaya, 50603 Kuala Lumpur, Malaysia
[b] Chemical Engineering Department, Faculty of Engineering, University of Malaya, 50603 Kuala Lumpur, Malaysia

ARTICLE INFO

Article history:
Received 17 May 2014
Received in revised form 24 October 2014
Accepted 5 November 2014
Available online 8 November 2014

Keywords:
Amine-functionalized ionic liquid
Guanidinium
Alkanolamine
CO_2 solubility
Physical property

ABSTRACT

It is an urgent act to limit greenhouse gas emissions to avoid the harmful effects of climate changes. In this work, the binary and ternary systems of guanidinium trifluoromethanesulfonate ([gua][OTf]) in *N*-methyldiethanolamine (MDEA) and/or water were examined as alternative solvents for gas treatment process. The thermodynamic properties including density, ρ, viscosity, η, thermal expansion, α_p and physical solubility of CO_2 in the systems were measured as a function of molar composition with a temperature range of 293.2–333.2 K at 100–1000 kPa. The presence of [gua][OTf] accelerates CO_2 absorption process. The present study offers equations of correlation providing a reliable prediction of the binary and ternary systems as a function of concentration. The linear equation, quadratic equation, extended Arhenius equation and Henry's Law equation have been applied to assess the validity of the finding. The CO_2 solubilities in [gua][OTf] systems are found higher compared to other ILs in previous researches. Additionally, ANN modeling of the effective parameters was carried out and the composition of [gua][OTf] was proven as the key factor in maximizing the CO_2 solubility.

1. Introduction

Amine scrubbing has been used to separate CO_2 from natural gas and hydrogen since 1930. It is a robust technology, well understood and widely used [1]. One of the most potent techniques widely used in capturing CO_2 from low pressure flue gas streams in power plants is chemical absorption using aqueous amine-based absorbents [2–4].

Furthermore, unprompted MDEA or alkali–carbonate solutions are very attractive as the solutions have high stability and are inexpensive [5]. The utmost benefits of MDEA are its high equilibrium loading capacity (about 1.0 mol of CO_2/mol of amine), the best selectivity under typical operating conditions encountered in the industry and low heat of reaction with the acid gases, which leads to lower energy requirement for regeneration [6–9]. On the other hand, MDEA has a low rate of reaction with (and therefore absorption of) CO_2. They are able to carry out a high total CO_2 removal, but at much lower rates [10–13]. Thus, new formulations comprising mixtures of amines with various additives are continuously being developed to overcome some of the drawbacks in their use and implementation.

It has been demonstrated previously that thermophysical properties have a substantial influence on the design of physicochemical processing and reaction units, especially the design parameters and performance of equipment like heat exchangers, distillation columns and reactors. To date, ionic liquids (ILs) have received an advantage in various applications including in CO_2 scrubbing [14–17]. ILs possess exceptional arrays of physical properties that make them suitable in numerous task-specific applications in which conventional solvents are ineffective, such as high heat capacity per unit volume, high thermal stability, high electrical conductivity, wide range of viscosity, very good solvent properties, and negligible vapor pressure [18–21].

Amine-based ILs as precursor liquids for CO_2 absorption was first discussed by Bates et al. [22] in 2002. Simple synthetic method and the use of commercially available starting materials are the highlight of this compound. However, the key problem of these task-specific ionic liquids (TSILs) is attributed to half-molar CO_2 uptake per one mole of IL. Likewise, the homogeneous ILs mainly suffers from gas diffusion limitation specially by increasing the viscosity of the CO_2-captured ILs. In our previous work, the solubility of CO_2 in aqueous blended system of MDEA and [gua][OTf] at partial pressure ranging from 500 to 3000 kPa were reported [23] . It has been found that the aqueous [gua][OTf] gave significantly higher solubility, up to 1.63 mol CO_2/mole absorbent, as compared to other pure ILs.

Abbreviations: IL, ionic liquid; [gua][OTf], guanidinium trifluoromethanesulfonate; MDEA, *N*-methyldiethanolamine; GC, gas chromatography; CO_2, carbon dioxide; ANN, artificial neural network.

* Corresponding author. Tel.: +60 3 79675160; fax: +60 3 79677188.
E-mail address: asrina@um.edu.my (N.A. Sairi).

http://dx.doi.org/10.1016/j.fluid.2014.11.009
0378-3812/

Nomenclature

ρ	density
η	viscosity
α_p	thermal expansion
E_a	activation energy

Empirical equations for the density and viscosity of pure components as a function of a temperature and composition were applied and compared with experimental data. These equations are useful for interpolation within the studied temperature range. On the other hand, the excess thermodynamic properties and non-thermodynamic ones were fitted to a Redlich–Kister type equation using least squares to obtain their dependency on concentration and temperature [24–26]. A simple correlation is proposed in this work due to limited experimental data.

The complexities of parameters behavior in [gua][OTf]–MDEA systems for low pressure CO_2 solubility might cause misinterpretation of the results. The complexities cause major challenges for conventional methods such as one-variable-one-time [27]. CO_2 solubility does not depend on any single parameter alone and a combination of parameters affects the absorption of CO_2. An artificial neural network (ANN) is a powerful tool for analyzing this dependency. As consequence, ANN could be a promising multivariate method which involved complicated statistical calculation such as fitting process and regression analysis [28,29]. The ANN models possessed reliable, robust and salient characteristics in capturing the non-linear relationships between variables in the complex systems such as chemical reaction processes [30,31].

Hence, the objectives of this work are reported in four parts. Firstly, to contribute to the databank of physical property, by measuring the density, dynamic viscosity and CO_2 solubility of [gua][OTf]–MDEA systems. Secondly, to examine the effect of [gua][OTf] addition to MDEA as a function of temperature. Thirdly, to create a correlation of density, dynamic viscosity and CO_2 solubility in function of concentration (unit in M) of MDEA and [gua][OTf] at temperatures 298–363 K. Finally, to predict the most affecting parameter involving in CO_2 solubility by the development of a multilayer feed-forward neural network model, ANN.

2. Methodology

2.1. Chemicals

Analytical reagents (AR), [gua][OTf] and MDEA (98.5% and 98.0% by mass, determined by HPLC and GC, respectively), used in this work were purchased from Merck. The molecular formula, IUPAC name, CASRN, sources, purity grade, mass fraction and analysis method of the components are listed in Table 1. The structures of the [gua][OTf] and MDEA are shown in Fig. 1(a) and (b), respectively. The distilled water was used with double distilled purification. No further purification was made for all the compounds. Other chemical reagents include: HCl, $BaCl_2$, NaOH, $NaHCO_3$ and CO_2 were used without further treatment. Sodium hydroxide (NaOH, 99.0% purity), barium chloride ($BaCl_2$, 99% purity), and sodium bicarbonate ($NaHCO_3$, 99.0% purity) were purchased from Merck. Purified carbon dioxide (CO_2, purity $\geq$99.995%) was supplied by Malaysian Oxygen Berhad (MOX). Standard solution of hydrochloric acid (HCl, 1.0 N) for titration was obtained from Fisher Chemicals.

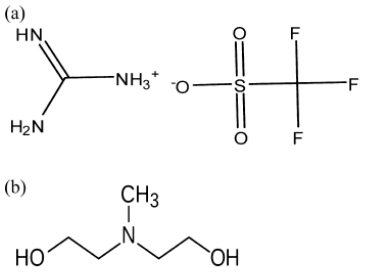

Fig. 1. (a) Structure of guanidinium trifluoromethanesulfonate, ([gua][OTf]) with molecular weight 209.15 g mol^{-1}. (b) Structure of *N*-methyldiethanolamine, (MDEA) with molecular weight 119.16 g mol^{-1}.

2.1.1. Sample preparation and validation

The compositions of the binary and ternary systems are shown in Table 2. All the systems were prepared gravimetrically and the accurate concentrations were determined by titration with 1.0 M HCl standard solution. All the systems used were found to be within 1% of the desired concentration.

2.2. Experimental setup and mode of operation

2.2.1. Density measurement

Density measurement of the binary and ternary systems was carried out with DMA- 4500 M (Anton Paar, Austria) digital densitometer thermostat at temperatures range of 273.2–363.2 K, with 10 K increment. The apparatus is precise within 1.0×10^{-5} g/cm^3, and the uncertainty of the measurements was estimated to be better than $\pm 1.0 \times 10^{-4}$ g/cm^3. The calibration of the densitometer was performed at atmospheric pressure using double-distilled and degassed water.

2.2.2. Viscosity measurement

Viscosity measurement was carried out using R/S+ rheometer (Brookfield, USA). The rheometer is a stress control (or controlled

Table 1
The sample provenance table for the compounds system.

Component	[gua][OTf]	MDEA
Molecular formula	$C_2H_6F_3N_3O_3S$	$CH_3N(CH_2CH_2OH)_2$
IUPAC name	Diaminomethylideneazanium; trifluoromethanesulfonate	2-[2-hydroxyethyl(methyl)amino]ethanol
CASRN	153756-25-3	511262-76-3
Source	Merck	Merck
Purity grade	AR	AR
Purity (mass fraction)	98.5	98.0
Purification method	None	None
Analysis method	HPLC	GC

Table 2
Compositions of binary and ternary systems.

System	Sample	Concentration, mol/dm^3		Mole fraction		
		MDEA	[gua][OTf]	x_{MDEA}	$x_{[gua][OTf]}$	x_{H2O}
Binary	4 M MDEA	4.005	0	0.1168	0	0.8832
	1 M MDEA	1.002	0	0.0192	0	0.9808
	4 M [gua][OTf]	0	4.003	0	0.2073	0.7928
	1 M [gua][OTf]	0	1.002	0	0.0202	0.9798
	0.9 M [gua][OTf]	0	0.900	0	0.0181	0.9820
	0.7 M [gua][OTf]	0	0.702	0	0.0137	0.9819
	0.5 M [gua][OTf]	0	0.503	0	0.0095	0.9905
	0.3 M [gua][OTf]	0	0.301	0	0.0056	0.9944
	0.1 M [gua][OTf]	0	0.102	0	0.0018	0.9982
Ternary	4 M MDEA + 2 M [gua][OTf]	4.004	2.002	0.1842	0.0903	0.7255
	4 M MDEA + 1 M [gua][OTf]	4.002	1.003	0.1416	0.0347	0.8237
	4 M MDEA + 0.9 M [gua][OTf]	4.002	0.904	0.1407	0.0310	0.8282
	4 M MDEA + 0.7 M [gua][OTf]	4.003	0.701	0.1342	0.0230	0.8427
	4 M MDEA + 0.5 M [gua][OTf]	4.001	0.503	0.1283	0.01570	0.8560
	4 M MDEA + 0.3 M [gua][OTf]	4.001	0.303	0.1229	0.0090	0.8681
	4 M MDEA + 0.1 M [gua][OTf]	4.001	0.102	0.1179	0.0029	0.8792
	3 M MDEA + 1 M [gua][OTf]	3.003	1.003	0.0931	0.03163	0.8753
	2 M MDEA + 2 M [gua][OTf]	2.001	2.004	0.0715	0.0728	0.8557
	1 M MDEA + 3 M [gua][OTf]	1.002	3.002	0.0424	0.1297	0.8279

Standard uncertainties: u are $u(T) = 0.01$ K; $u(x) = 0.0001$ and $u(P) = 1$ k Pa.

torque) instrument and was calibrated using standard viscosity oil. The temperature of the solution was maintained within ±0.1 K. The viscosities were measured with the accuracy less than 1%. All the measurements for each sample were performed in triplicate, and the values were reported as an average. The measurement was taken at atmospheric pressure and temperature range of 298.2–363.2 K, with 10 K increment.

2.2.3. Physical solubility at low pressure

The double jacket stirred cell reactor was equipped with a pressure transducer, thermocouple, a magnetic stirrer, and a pH meter which was linked to a data acquisition system. A schematic diagram of the experimental set-up used in this work was shown in Fig. 2, similar to the one used by Aroua et al., in 1998 [32]. The experiments were conducted at 303.2 K under 1 atm with flow rates CO_2: total gas, 10%, 50% and 100% ratio constantly 2000 ml/min flow rate. The auto titrator was incorporated with the measurement equivalence-point titration (MET) technique for the determination of endpoint of pH.

2.2.3.1. Determination of amine concentration. At the beginning and end of each experiment, 10 ml of all the samples were titrated with the standard solution of 1 M HCl to verify that the concentration of the samples has not changed throughout the experiment.

2.2.3.2. Determination of CO_2 loading. The samples of carbonated systems were taken and mixed with $BaCl_2$ and NaOH. $BaCO_3$ precipitated was then added to the distilled water. The $BaCO_3$ solution was titrated with the standard solution of 1 M HCl using Metrohm 716 DMS Titrino auto titrator, which utilizes the Dynamic Equivalence-point Titration (DET) technique for the determination of the end point. The method of determining CO_2 loading viatitration is ascertained and verified by conducting similar

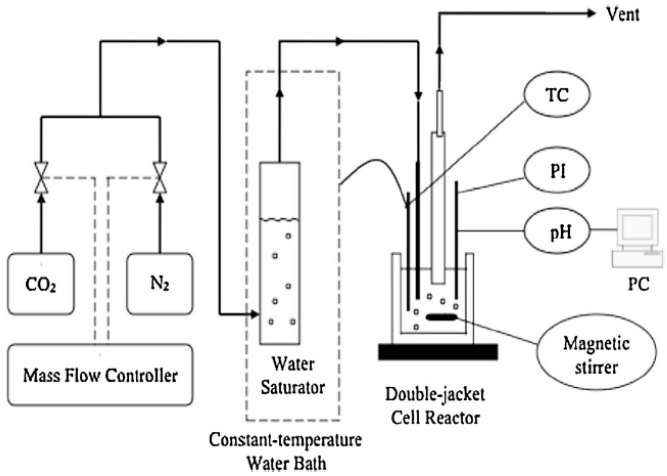

Fig. 2. Schematic diagram of the experimental set-up.

experiment on samples containing a known amount of $NaHCO_3$. The tests were done in triplicate for each sample.

2.2.3.3. Data analysis. The volume of HCl was used to neutralize the basic species in the solution determined from the end points exploiting the first derivative of the titration curve. The CO_2 loading of the solution is defined as total mole of CO_2 absorbed per mole of absorbent. It can be calculated by using the following equation:

$$CO_2 \text{loading}, \alpha = \frac{V_{HCl}}{2[MDEA](V_{sample})} \quad (1)$$

where α: CO_2 loading in mole of CO_2 per mole of absorbent; V_{HCl}: volume of HCl needed to neutralize the basic species in ml; V_{sample}: volume of sample taken for analysis in ml; M: molarity of the alkanolamine solution in mole per liter.

3. Results and discussion

3.1. Validation of data

The validation of data using pure MDEA was carried out to ensure the accuracy of the measurements used in this work. These experimental data of pure compound and comparisons with the literature reviews [33–35] were presented in Table 3. There is a good agreement between the measured densities of pure MDEA in this work, Rebolledo-Libreros and Trejo [33] and Zhao et al. [34] with an average absolute deviation of 0.20%. Meanwhile, the viscosities of pure MDEA obtained in this work is in agreement with those reported by Zhao et al. [34] and Bernal-Garcia et al. [35] with average deviation of ±0.05%. The approach of this work on CO_2 solubility was identical to Benamor and Aroua [36]. The data deviation between their results and this work for aqueous 4 M MDEA on CO_2 loading was less than 2%.

Good corresponding with the literature data [36–40] was observed for aqueous 1 M and 4 M MDEA as shown in Figs. 3–5 on density, viscosity and CO_2 solubility.

The results shown in Table 4 pointed out that the presence of IL did not interfere with CO_2 solubility measurement. Thus, the chemical approach practiced in this research for the measurement of CO_2 solubility in low pressure (≤100 kPa) for alkanolamines was still relevant to the systems involving ILs. According to the similar titration curves, the presence of IL did not interfere with the titration results.

3.2. Density

The measured densities of the binary and ternary systems throughout the whole temperature range from 298.2–363.2 K were plotted in Figs. 6 and 7. The density curves showed a quasi-linear decrease in values for all binary and ternary systems. It can be seen from Fig. 6 that the density of 1 M [gua][OTf] was higher by

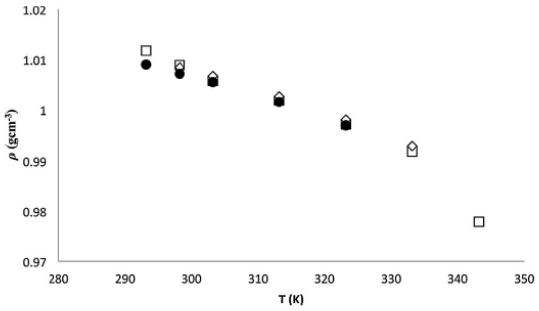

Fig. 3. Density of aqueous 1 M MDEA as function of temperatures. (□) this work; (◇) Muhammad et al. [37]; (●) Derks et al. [38].

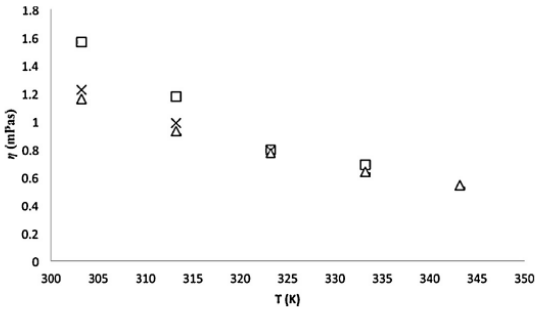

Fig. 4. Viscosity of aqueous 1 M MDEA as function of temperatures. (□) this work; (×) Derks et al. [38]; (-) Teng et al. [39]; (△) Arachchige et al. [40].

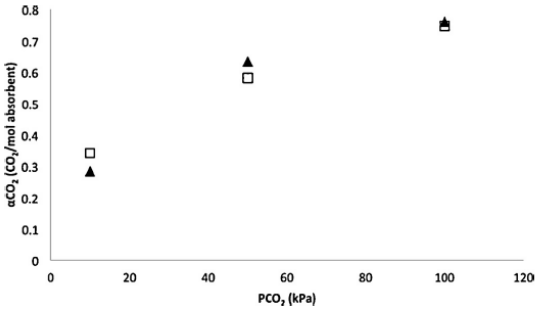

Fig. 5. CO_2 solubility of aqueous 4 M MDEA as function of CO_2 partial pressures. (□) this work; (Δ) Benamor and Aroua [36].

Table 3
Comparison of density and viscosity for pure MDEA and CO_2 solubility for aqueous 4 M MDEA at different temperature, atmospheric pressure.

	T/K	This work	Rebolledo-Libreros and Trejo [33]	Zhao et al. [34]	Bernal-Garcia et al. [35]	Benamor and Aroua et al. [36]
Density, ρ (g/cm^3)	313.2	1.0267	1.0171	1.0264	–	–
	323.2	1.0189	1.0115	1.0190	–	–
	333.2	–	1.0041	–	–	–
Viscosity, η (mPa s)	303.2	56.30	–	57.5	57.57	–
	313.2	34.44	–	35.0	34.78	–
	323.2	22.93	–	22.0	21.98	–
CO_2 loading(mol CO_2/mol absorbent)	303.2	0.748	–	–	–	0.761
	323.2	0.645	–	–	–	0.654

Standard uncertainties: u are $u(T) = 0.01$ K; $u(x) = 0.0001$ and $u(P) = 1$ kPa. Relative standard uncertainty: u_r are $u_r(\rho) = 0.001$ and $u_r(\eta) = 0.03$.

Table 4
Validation experiments on 4 M MDEA system at 303.2 K with the presence of 100% CO_2 containing a known amount of $NaHCO_3$ at atmospheric pressure.

Solution	4 M MDEA + $NaHCO_3$	4 M MDEA + 1 M [gua][OTf] + $NaHCO_3$
CO_2 loading to be verified (mol CO_2/mol MDEA)	0.5	0.5
Mol of $NaHCO_3$ in 5 ml sample	0.02	0.02
Calculated V_{HCl} (ml)	20	20
Actual V_{HCl} (ml)	20.094	20.161
Deviation, %	0.47	0.81

Standard uncertainties: u are $u(T) = 0.01$ K, $u(x) = 0.0001$ and $u(P) = 1$ k Pa.
M: concentration, mol/dm^3.

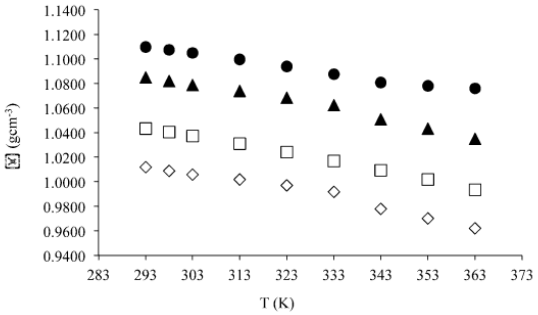

Fig. 6. Density of the binary systems at different molar fraction as function of temperatures. (□) 4 M MDEA; (◇) 1 M MDEA; (●) 4 M [gua][OTf]; (▲) 1 M [gua][OTf].

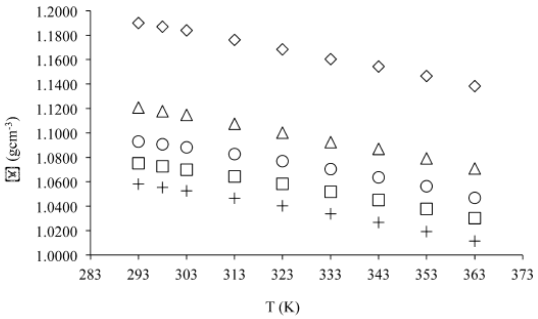

Fig. 7. Density of the ternary systems at different molar fraction as function of temperatures. (◇) 4 M MDEA + 2 M [gua][OTf]; (△) 4 M MDEA + 1 M [gua][OTf]; (+) 3 M MDEA + 1 M [gua][OTf]; (□) 2 M MDEA + 2 M [gua][OTf]; (○) 1 M MDEA + 3 M [gua][OTf].

7.26% than 1 M MDEA in the temperature range considered. Similarly, the density varied 6.52% between 4 M [gua][OTf] and 4 M MDEA. The density values of the binary systems studied followed this sequence: 4 M [gua][OTf] > 1 M [gua][OTf] > 4 M MDEA > 1 M MDEA.

Fig. 7 shows that the density sequence followed the order of 4 M MDEA + 2 M [gua][OTf] > 4 M MDEA + 1 M [gua][OTf] > 1 M MDEA + 3 M [gua][OTf] > 2 M MDEA + 2 M [gua][OTf] > 3 M MDEA + 1 M [gua][OTf]. The composition of [gua][OTf] highly influenced density of the systems compared to MDEA. This has been proven by the density value of 1 M MDEA + 3 M [gua][OTf] being higher than 2 M MDEA + 2 M [gua][OTf] and 3 M MDEA + 1 M [gua][OTf]. The divergence of [gua][OTf] composition gave substantial increment between 4 M MDEA + 1 M [gua][OTf] and 4 M MDEA + 2 M [gua][OTf]. This is due to the high molecular weight of [gua][OTf] at 209.15 g mol^{-1}.

All the systems showed that the density linearly decreased with increasing the temperature. This indicated that the kinetic energy of molecules and the volume between molecules are increasing when the temperature is increased. Therefore, the interactions between molecules decrease, so the contraction in volume decreases and this leads to the decreasing of density with increment in the temperature. In specific volume, the amount of water contained in solution mixture decreased as the concentration increased. It is known that water in the blend of [gua][OTf]–MDEA appeared to act as a diluent, thus it lowers the density of the system. The studied [gua][OTf]–H_2O was also compared with [hmim][Br]–H_2O [41] and [BuPy][BF_4]–H_2O [42] with the composition of IL at 0.5 mol fractions, respectively. Fig. 8 shows that the [gua][OTf]–H_2O has lower densities compared to [hmim][Br]–H_2O and [BuPy] [BF_4]–H_2O at the same temperature range.

A correlation relating the binary systems and ternary systems with temperature from 293.2–363.2 K can be expressed using the following linear equation (Eq. (2)) [43,44]. The values of α and β are summarized in Table 5.

$$\rho(\mathrm{g cm^{-3}}) = [\beta((\mathrm{g cm^{-3}})K) \times T(K)] + \alpha(\mathrm{g cm^{-3}}) \quad (2)$$

From Table 5, 1 M [gua][OTf] exhibits highest α value followed by 4 M MDEA + 2 M [gua][OTf]. As for 4 M MDEA and 1 M MDEA, the α value increased as the concentration of MDEA increased. Meanwhile, the α value decreased as the concentration of [gua][OTf] increased. It is observed that there was an increment trend for the ternary systems as the α value increased from 1 M MDEA + 3 M [gua][OTf] < 2 M MDEA + 2 M [gua][OTf] < 3 M MDEA + 1 M [gua][OTf] < 4 M MDEA + 1 M [gua][OTf] < 4 M MDEA + 2 M [gua][OTf]. The R^2 values obtained for all the systems were very close to unity, which further enhanced the precision of correlation in Eq. (2) to be used as estimation for the densities within temperature range from 293.2–363.2 K.

A quadratic equation relating characteristic parameter,β, with the concentration of [gua][OTf] is expressed as below:

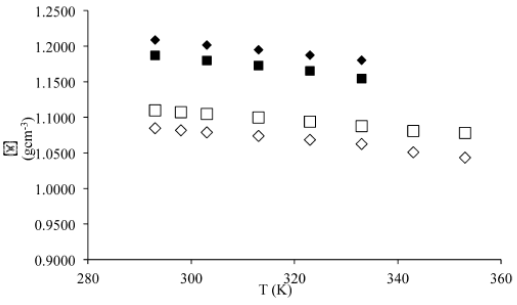

Fig. 8. Comparison in density between [gua][OTf]–H_2O i.e., 4 M [gua][OTf] and 1 M [gua][OTf] with [hmim][Br]–H_2O [41] and [BuPy][BF_4]–H_2O [42]. (□) 4 M [gua][OTf]; (◇) 1 M [gua][OTf]; (◆) [hmim][Br]–H_2O; (■) [bmim] BF_4]–H_2O.

Table 5
Calculated and measured density data for studied systems at atmospheric pressure with α and β values.

Sample	α	β	T	Correlation data ($g\,cm^{-3}$)	Experimental data ($\pm 1.0 \times 10^{-4}\,g\,cm^{-3}$)	Deviation, %
4 M MDEA +2 M [gua][OTf]	1.4086	−0.000737	293.2	1.1927	1.1899	−0.230
			298.2	1.1890	1.1870	−0.167
			303.2	1.1853	1.1839	−0.121
			313.2	1.1780	1.1762	−0.150
			323.2	1.1705	1.1683	−0.190
			333.2	1.1632	1.1603	−0.249
			343.2	1.1558	1.1542	−0.136
			353.2	1.1484	1.1465	−0.166
			363.2	1.1411	1.1383	−0.240
4 M MDEA +1 M [gua][OTf]	1.3304	−0.000708	293.2	1.1230	1.1207	−0.197
			298.2	1.1194	1.1178	−0.143
			303.2	1.1159	1.1147	−0.107
			313.2	1.1088	1.1075	−0.118
			323.2	1.1017	1.1001	−0.147
			333.2	1.0946	1.0924	−0.207
			343.2	1.0876	1.0868	−0.070
			353.2	1.0805	1.0791	−0.131
			363.2	1.0734	1.0709	−0.236

Sample	α	β	T	Correlation data ($g\,cm^{-3}$)	Experimental data ($\pm 1.0 \times 10^{-4}\,g\,cm^{-3}$)	Deviation, %
4 M MDEA	1.2522	−0.000707	293.2	1.0451	1.0433	−0.164
			298.2	1.0415	1.0404	−0.106
			303.2	1.0380	1.0373	−0.067
			313.2	1.0309	1.0308	−0.008
			323.2	1.0238	1.0241	0.023
			333.2	1.0168	1.0169	0.013
			343.2	1.0097	1.0094	−0.030
			353.2	1.0026	1.0017	−0.097
			363.2	0.9956	0.9935	−0.211
3 M MDEA +1 M [gua][OTf]	1.2610	−0.00070475	293.2	1.0545	1.0580	0.329
			298.2	1.0510	1.0553	0.412
			303.2	1.0475	1.0525	0.484
			313.2	1.0404	1.0467	0.599
			323.2	1.0333	1.0404	0.678
			333.2	1.0263	1.0337	0.716
			343.2	1.0193	1.0266	0.722
			353.2	1.0122	1.0192	0.691
			363.2	1.0052	1.0114	0.622

Sample	α	β	T	Correlation data ($g\,cm^{-3}$)	Experimental data ($\pm 1.0 \times 10^{-4}\,g\,cm^{-3}$)	Deviation, %
2 M MDEA +2 M [gua][OTf]	1.2426	−0.000733	293.2	1.0278	1.0751	4.597
			298.2	1.0242	1.0726	4.727
			303.2	1.0205	1.0700	4.847
			313.2	1.0132	1.0644	5.055
			323.2	1.0058	1.0584	5.221
			333.2	0.9985	1.0519	5.345
			343.2	0.9912	1.0451	5.436
			353.2	0.9839	1.0378	5.483
			363.2	0.9765	1.0302	5.496
1 M MDEA +3 M [gua][OTf]	1.2312	−0.00075725	293.2	1.0093	1.0930	8.294
			298.2	1.0055	1.0907	8.467
			303.2	1.0018	1.0882	8.628
			313.2	0.9942	1.0827	8.903
			323.2	0.9866	1.0768	9.141
			333.2	0.9790	1.0705	9.337
			343.2	0.9715	1.0637	9.493
			353.2	0.9639	1.0563	9.587
			363.2	0.9563	1.0469	9.472

Sample	α	β	T	Correlation data ($g\,cm^{-3}$)	Experimental data ($\pm 1.0 \times 10^{-4}\,g\,cm^{-3}$)	Deviation, %
1 M MDEA	1.2486	−0.000731	293.2	1.0344	1.0118	−2.185
			298.2	1.0308	1.0089	−2.122
			303.2	1.0271	1.0058	−2.078
			313.2	1.0198	1.0018	−1.797
			323.2	1.0125	0.9971	−1.544
			333.2	1.0052	0.9918	−1.351
			343.2	0.9979	0.9779	−2.003
			353.2	0.9906	0.9701	−2.061
			363.2	0.9833	0.9620	−2.167
4 M [gua][OTf]	1.2610	−0.000743	293.2	1.0433	1.1096	5.975
			298.2	1.0396	1.1073	6.114

Table 5 (*Continued*)

Sample	α	β	T	Correlation data ($g\,cm^{-3}$)	Experimental data ($\pm 1.0\times10^{-4}\,g\,cm^{-3}$)	Deviation, %
			303.2	1.0359	1.1049	6.245
			313.2	1.0284	1.0996	6.475
			323.2	1.0210	1.0938	6.656
			333.2	1.0136	1.0875	6.795
			343.2	1.0062	1.0808	6.902
			353.2	0.9987	1.0779	7.348
			363.2	0.9913	1.0759	7.863
Sample	α	β	T	Correlation data ($g\,cm^{-3}$)	Experimental data ($\pm 1.0\times10^{-4}\,g\,cm^{-3}$)	Deviation, %
1 M [gua][OTf]	1.294	−0.000722	293.2	1.0825	1.0848	0.212
			298.2	1.0788	1.0819	0.287
			303.2	1.0752	1.0788	0.334
			313.2	1.0680	1.0739	0.548
			323.2	1.0608	1.0684	0.711
			333.2	1.0536	1.0623	0.819
			343.2	1.0464	1.0509	0.434
			353.2	1.0391	1.0432	0.386
			363.2	1.0319	1.0350	0.294

Standard uncertainties: u are $u(T) = 0.01$ K, $u(x) = 0.0001$ and $u(P) = 1$ k Pa. Relative standard uncertainty, u_r are $u_r(\rho) = 0.001$. M: concentration, mol/dm^3.

$$-\beta \times 10^{-4} = a([\text{gua}][\text{OTf}])^2 + b[\text{gua}][\text{OTf}] + c \quad (3)$$

where $a = 0.14$; $b = -0.0575[\text{MDEA}]^2 + 0.355\ [\text{MDEA}] - 0.63$; $c = 0.08\ [\text{MDEA}]^2 - 0.48[\text{MDEA}] + 7.71$.

Another quadratic equation relating characteristic parameter,α, with the concentration of [gua][OTf] is then expressed as below:

$$\alpha = p([\text{gua}][\text{OTf}])^2 + q[\text{gua}][\text{OTf}] + r \quad (4)$$

where $p = 2 \times 10^{-5}$; $q = 0.0057\ [\text{MDEA}]^2 - 0.0005[\text{MDEA}] - 0.011$; $r = 0.0144\ [\text{MDEA}]^2 - 0.0708[\text{MDEA}] + 1.305$.

Fig. 9 shows the comparison between the calculated and the experimental density for 4 M MDEA + 2 M [gua][OTf], 4 M MDEA + 1 M [gua][OTf], 3 M MDEA + 1 M [gua][OTf], 4 MDEA and 1 M [gua][OTf]. The percentages deviations of the calculated densities for these systems were less than ± 1% in the temperature range from 293.2–363.2 K. The deviation for 1 M MDEA was less than 2%. However, systems with 2 M [gua][OTf] and higher, have shown deviation up to 9.587%.

3.3. Thermal expansion

Table 6 shows that the changes in the coefficients of thermal expansion values and the variation of volume expansion of the studied systems are dependent on temperature. Since the densities decreased linearly with temperature, it is obvious that α_p values are all positive but slightly increases with temperature. Similar trends of densities are observed for the thermal expansion coefficients. The values of α_p increased from 6.1795×10^{-6} to $7.9184 \times 10^{-6}\,K^{-1}$ with increasing of [gua][OTf] composition in the systems. The coefficients of thermal expansion values for the systems studied in this work are calculated based on the measured density data using Eq. (5) .

$$\alpha_p = \frac{-1}{\rho}\left(\frac{\partial \rho}{\partial T}\right)_p = \frac{-\beta}{(\alpha + \beta T)} \quad (5)$$

where α_p is the coefficient of thermal expansion, ρ, is the density, T is the temperature and α and β are the correlation coefficients obtained from Eq. (3) by fitting the measured density data.

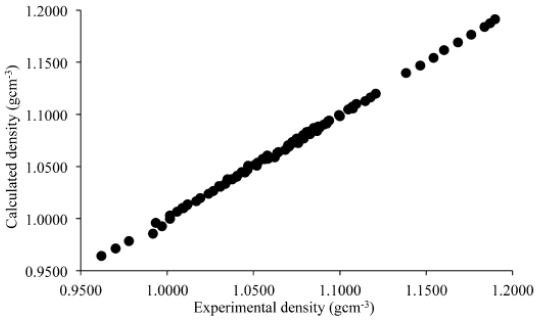

Fig. 9. Density comparison between calculated and measured density of 4 M MDEA + 2 M [gua][OTf], 4 M MDEA + 1 M [gua][OTf], 3 M MDEA + 1 M [gua][OTf], 4 MDEA and 1 M [gua][OTf].

3.4. Dynamic viscosities

Tables 7 and 8 show the viscosities of the systems demonstrate a temperature-dependent behavior. The viscosities decrease exponentially as the temperature increases. Fig. 10 shows the viscosities of various compositions of [gua][OTf]–H_2O at the temperature range between 293.2 and 333.2 K. It can be seen that there is a large difference of viscosities between the systems at different composition of [gua][OTf]. However, as the temperature approaches 333.2 K, the difference in the viscosities of all the systems became negligible.

Fig. 11 shows that at fixed temperature, the viscosity of ternary systems increases as the concentration of [gua][OTf] increases. This is due to the interactions between the solute molecules i.e., [gua][OTf] and the organic liquid solvent, MDEA. This phenomenon could be explained by the increase of the hydrogen bonding force between [gua][OTf] and MDEA, which leads to the increase in the viscosity of the systems.

The addition of [gua][OTf] into the solution of MDEA–H_2O would reduce the overall viscosity of the systems. Moreover the presence of water, which is known, to have low viscosity is another factor for the viscosity reduction. Some studies reported that water would accommodate in the ILs structure possibly by forming hydrogen bonds with both anion and cation. The dramatic decrease in viscosity was due to the fact that the water molecules reduce the electrostatic attractions between the ions. Thus, the overall cohesive energy of the systems is lowered.

Fig. 12 shows the viscosity of [bmim][BF_4]–H_2O [45] and [gua][OTf]–H_2O based on mole fraction of IL at 298.2 K. It can be seen that the viscosity of the IL systems strongly depends on their concentration. The viscosities of the binary systems are lower than [bmim][BF_4]–H_2O system.

Link to Full-Text Articles :

http://www.sciencedirect.com/science/article/pii/S0378381214006463